J. COMBIN. MATH. COMBIN. COMPUT. 127b (2025) 5125--5148

Journal of Combinatorial Mathematics
and Combinatorial Computing
www.combinatorialpress.com/jcmcc

Integrated electromagnetic and noise optimization design of Fe-based soft magnetic composite core reactor based on genetic algorithm

Yangyang Ma[1], Wenle Song[1], Jie Gao[2,✉], Yang Liu[2], Yilei Shang[2], Weimei Zhao[2], Fuyao Yang[2]

[1] *State Grid Cangzhou Electric Power Supply Company, Cangzhou, Hebei, 061000, China*

[2] *China Electric Power Research Institute, Beijing, 100192, China*

ABSTRACT

Fe-based soft magnetic composites are widely used in power electronics and power system equipment due to their excellent magnetic properties and low iron loss. As a key component, the performance of the core reactor directly affects the operation efficiency and stability of the power system, and the traditional design method is difficult to take into account the electromagnetic performance and noise control at the same time. In this study, genetic algorithm is used to co-optimize the core structure, electromagnetic parameters and noise characteristics to reduce losses, improve electromagnetic compatibility, and reduce the noise generated during operation. In terms of methodology, a multi-physical field calculation model is constructed based on finite element analysis, electromagnetic performance and noise source characteristics are simulated, and genetic algorithm is used to optimize the parameter combinations under the constraints to form an optimized design scheme. During the optimization process, a suitable objective function is selected and combined with a multi-objective optimization strategy to balance the electromagnetic performance and noise suppression effect. The results show that the optimized core reactor is better than the traditional design in terms of loss, magnetic field distribution and noise level. The optimization scheme derived from the study can effectively improve the electromagnetic characteristics of the equipment and significantly reduce the noise level, providing strong support for the design and improvement of related equipment.

Keywords: Fe-based soft magnetic composites; core reactor; genetic algorithm; constraints; optimization design

✉ Corresponding author.
E-mail address: conch3501@163.com (J. Gao).
Received 03 March 2024; Revised 20 April 2024; Accepted 10 November 2024; Published Online 16 April 2025.
DOI: 10.61091/jcmcc127b-285
© 2025 The Author(s). Published by Combinatorial Press. This is an open access article under the CC BY license (https://creativecommons.org/licenses/by/4.0/).

1. Introduction

With China's explicitly stated goals of peak carbon and carbon neutrality, clean energy related technologies such as wind power and photovoltaic have been rapidly developed in China [1-2]. With the subsequent large-scale application of power electronics and other nonlinear devices, the application of power electronics and other nonlinear devices can bring serious interharmonic pollution to the power grid, which not only affects the external environment and the surrounding population, but also affects the reactor itself [3-6]. At the same time, with the large number of power electronic devices, the impact of grid intermediate harmonics on power equipment is becoming more and more serious, and the interharmonics will aggravate the noise pollution of the power core reactor. Therefore, it is of great scientific significance and engineering value to study the electromagnetic and noise optimization of the core reactor [7-10].

The optimal design of the core reactor refers to the determination of a certain objective under the condition of satisfying the specified electromagnetic performance indexes, and the application of certain optimization algorithms to seek out the optimal product design scheme [11-12]. Traditionally, empirical algorithms are used to repeatedly adjust the design parameters such as core diameter, wire size, number of parallel roots and number of turns, etc. It is time-consuming and laborious, and it cannot achieve the optimal overall performance [13-16]. Genetic algorithm is a widely used and efficient stochastic search and optimization method based on the principles of evolutionary theory, with few restrictions and requirements on the solved optimization problem and its robustness and implied parallelism make it effective for global search in a probabilistic sense [17-20]. In particular, it provides great flexibility for optimization of various special problems through the diversity of its hybrid domain constructs, and thus is increasingly used [21-22].

After combing the magnetic performance parameters of Fe-based soft magnetic composites, the article applies them to the design of the core reactor and explores the vibration and noise characteristics of the Fe-based soft magnetic composite core reactor by combining the magnetostrictive force and Maxwell's force. The finite element simulation model of the Fe-based soft magnetic composite core reactor is established by combining finite element software with electromagnetic field, structural force field and acoustic field. A hierarchical optimization model is constructed and a genetic algorithm is introduced for optimization and solution to realize the vibration and noise structural optimization of the Fe-based soft magnetic composite core reactor. Finally, the performance of the Fe-based soft magnetic composite core reactor is simulated and analyzed, and the optimization results of the structural parameters are verified.

2. Fe-based soft magnetic composite core reactors

The core reactor is characterized by simple structure, high reliability, and can be used to absorb grid harmonics and improve the system voltage waveform. In recent years, the reactor has been overheating or even catching fire during operation, and one of the main reasons is that the electromagnetic vibration in the coil area is too high. When the electromagnetic vibration exceeds the limit, the insulation and mechanical properties of the material are significantly reduced, directly affecting the safety and stability of the reactor. At present, methods such as increasing the cross-section of the wire and the width of the air channel are usually used to reduce the electromagnetic vibration, but this will lead to an increase in the amount of metal conductor, and at the same time does not take into account the effect of the coil structural adjustment on the electromagnetic characteristics and vibration characteristics. Therefore, in order to improve the utilization rate of coil metal materials and reduce the manufacturing cost, Fe-based soft magnetic composites are introduced to optimize the structural design of the core reactor, and the electromagnetic, vibration and noise characteristics of the core reactor incorporating Fe-based soft magnetic composites are deeply explored and the optimization method of balanced regulation is proposed.

2.1. Parameters of magnetic properties of soft magnetic composites

2.1.1. Magnetic induction and permeability:

1) Saturation magnetic induction. The magnetic core will be magnetized under the action of the magnetic field, and its internal magnetic domains rotate slowly. When the core is completely magnetized, the direction of the magnetic domains and the applied magnetic field are all the same, even if the external magnetic field is increased, the magnetic domains are no longer rotating, and the inductor enters into a saturated state, and at this time, the corresponding magnetic induction strength is the saturated magnetic induction strength [23]. Its size can be expressed as:

$$B=\mu_0(H+M) \tag{1}$$

Where μ_0 is the vacuum permeability, H is the applied magnetic field strength, and M is the magnetization strength.

It is generally believed that the higher the saturation magnetic induction strength, the more energy can be stored per unit volume (i.e., energy density), in the design of the relevant magnetic device requires a smaller volume, more conducive to the miniaturization of the device.

For inductors, after saturation, the induced magnetic field strength no longer increases with the increase in applied current, the inductive potential of the coil can not effectively resist the applied potential, so that the coil current rises rapidly, resulting in overheating of the coil, which can cause the coil to burn up in severe cases. Therefore, in the selection process of inductors need to strictly consider the inductance saturation parameters. In addition to soft magnetic powder, the insulation layer will also affect the saturation magnetization strength of the core. Namely:

$$M_S=\frac{M_{SP}\cdot V_P+M_{SL}\cdot V_L}{V_p+V_L}=M_{SP}-\frac{6t}{d}(M_{SP}-M_{SL}) \tag{2}$$

Where, M_S is the saturation magnetic induction strength of the magnetic powder after coating, d is the effective diameter of the magnetic powder, t is the thickness of the insulating layer, V_R is the volume of the magnetic powder, V_L is the volume of the insulating layer, M_{SP} is the saturation magnetic induction strength of the magnetic powder, and M_{SL} is the saturation magnetic induction strength of the insulating layer.

In order to ensure high resistivity while preparing a thin and uniformly dense insulating layer, reducing the volume fraction of non-magnetic substances is the key to obtain a high saturation magnetization strength magnetic powder core.

2) Magnetic permeability. Magnetic permeability is a magnetic quantity that characterizes the magnetic conductivity of the magnet and the ease of magnetization, expressed as the ratio of the magnetic induction strength B and the magnetic field strength H. The magnetic permeability is the ratio of the magnetic induction strength B to the magnetic field strength H. That is:

$$\mu_{\text{absolutely}}=\frac{B}{H} \tag{3}$$

Magnetic powder core permeability decreases with the increase of application frequency, mainly due to the large increase of eddy currents in soft magnetic composites in high frequency alternating magnetic field, and its induced magnetic field will hinder the effective magnetization process of the applied magnetic field and reduce the magnetic permeability. Therefore, the frequency stability of magnetic powder core permeability can be effectively improved by improving the insulating cladding effect of the cladding layer, increasing the magnetic powder core resistivity, and reducing the eddy currents at high frequencies.

2.1.2. Magnetic Loss and Quality Factor Q:

1) Magnetic loss. Magnetic loss refers to the energy loss generated by the magnetic powder core in the alternating magnetic field. In the magnetic powder core working process, the magnetic loss is mostly dissipated in the form of heat, so the excessive magnetic loss is related to the heat resistance of the magnetic powder core. Magnetic loss P_{cv} consists of hysteresis loss P_h, eddy current loss P_e and residual loss P_{ex}. Where the residual loss refers to all other losses except hysteresis loss and eddy current loss, although there are various factors that cause residual loss, they can all be explained by the magnetization relaxation process.

Hysteresis loss refers to the energy loss caused by the hysteresis phenomenon when a magnetic material is magnetized in an alternating magnetic field. When the applied magnetic field is small, the magnetization is reversible, and the hysteresis loss is small at this time, but when the strength of the external magnetic field increases to the point where the magnetization is irreversible, the hysteresis loss increases rapidly. It can be expressed as:

$$P_h = K_h B_m^{\alpha} f \tag{4}$$

Where K_h is the hysteresis coefficient, B_m is the maximum induction, f is the frequency and α is the analog coefficient. It is proportional to the hysteresis coefficient K_h, the magnetic induction B_m^{α} and the operating frequency f, where the hysteresis coefficient and the analog coefficient are related to the coercivity of the material. Therefore, the reduction of hysteresis loss can be achieved by reducing the coercivity by reducing the impurities in the magnetic powder material and annealing heat treatment.

Eddy current loss refers to the loss formed when the magnetic powder core generates induced current internally in an alternating magnetic field, the induced current forms eddy currents within the magnetic powder particles, and the eddy currents pass through the conductor. As the induced current increases, the current between the magnetic powder particles conducts with each other to form the inter-particle eddy current, so the eddy current loss can be divided into the intra-particle eddy current loss and the inter-particle eddy current loss. It can be expressed as:

$$P_e = P_{intra} + P_{inter} = \left(\frac{d_{eff}^2}{\beta \rho_{SMCs}} + \frac{d}{20\rho_{powder}}\right)\pi^2 B_m^2 f^2 \tag{5}$$

where d_{eff} is the vortex effective size, d is the powder diameter, β is the geometric coefficient, and ρ_{SMCs} and ρ_{powder} are the body resistivity of the magnetic ring and the original powder, respectively. It is proportional to the square of the magnetic induction strength B_m and the square of the operating frequency f. The eddy current loss inside the particles can be reduced by reducing the powder particle size, and the eddy current loss between the particles can be effectively reduced by increasing the body resistivity of the magnetic powder core.

2) Quality factor Q. The quality factor is a performance index that reacts to the energy storage and loss of the magnetic powder core during AC magnetization. The test frequency of magnetic loss is generally not higher than 500kHz, so it can not be used to characterize the loss of the magnetic powder core at high frequency, so the quality factor is generally used to characterize the advantages and disadvantages of the magnetic powder core's soft magnetic performance at high frequency. In industrial production, the quality factor at 1MHz is generally used as a reference value, and the larger the value of the quality factor, the better the high-frequency soft magnetic performance.

Can be characterized by the ratio of inductance L_5 and equivalent loss resistance R_s at different frequencies, then:

$$Q = \frac{\mu'}{\mu^n} = \left(\frac{2\pi f L_s}{R_s}\right) \tag{6}$$

where μ is the real part of the permeability, μ' is the imaginary part of the permeability, f is the frequency, L_S is the inductance, and R_s is the equivalent resistance.

2.2. Soft magnetic composite core reactors

2.2.1. Structural parameters of core reactors. A Fe-based soft magnetic composite core reactor consists of a number of packages connected in parallel, each with several layers of coils connected in parallel, with each branch in its equivalent circuit corresponding to each layer of coils in the reactor. This contains the resistance R_i and self-inductance L_i of the coils, and the mutual inductance M_{ij} between the branches. When a turn-to-turn short-circuit occurs in layer m, the short-circuit ring is embodied as a single-turn closed loop on the equivalent circuit, which is recorded as layer $n+1$, and its resistance and self-inductance are recorded as R_{n+1}, L_{n+1}, and there is also mutual inductance between the short-circuit ring and each branch circuit $M_i(n+1)$ [24].

According to the equivalent circuit, the nodal voltage equation of the Fe-based soft magnetic composite core reactor can be listed as:

$$Z \times I^T = U^T \tag{7}$$

Where Z is the impedance matrix of the reactor, I is the current matrix of each branch of the reactor, and U is the voltage matrix of each branch of the reactor. The above equation can also be expressed when the reactor is in normal operation:

$$\begin{bmatrix} R_1 + j\omega L_1 & M_{12} & \cdots & M_{1n} \\ M_{12} & R_1 + j\omega L_1 & \cdots & M_{2n} \\ \vdots & \vdots & & \vdots \\ M_{1n} & M_{2n} & \cdots & R_n + j\omega L_n \end{bmatrix} \begin{bmatrix} I_1 \\ I_2 \\ \vdots \\ I_n \end{bmatrix} = \begin{bmatrix} U \\ U \\ \vdots \\ U \end{bmatrix} \tag{8}$$

When a turn-to-turn short-circuit occurs in layer m of the reactor, a closed short-circuit loop is added inside the reactor, i.e., layer $n+1$, which has a branch voltage of 0. Then the impedance matrix under a turn-to-turn short-circuit fault is denoted as Z_s, and:

$$Z_s = \begin{bmatrix} R_1 + j\omega L_1 & \cdots & M_{1n} & M_{1(n+1)} \\ \vdots & & \vdots & \vdots \\ M_{1n} & \cdots & R_n + j\omega L_n & M_{n(n+1)} \\ M_{1(n+1)} & \cdots & M_{n(n+1)} & R_{n+1} + j\omega L_{n+1} \end{bmatrix} \tag{9}$$

Considering the impedance of the short-circuited turn itself and the mutual inductance with other layers of coils, the impedance matrix changes accordingly, and the number of equations for the reactor changes to $n+1$ at this time. The current and voltage matrices change accordingly:

$$I = \begin{bmatrix} I_1 & I_2 & \cdots & I_n & I_{n+1} \end{bmatrix} \tag{10}$$

$$U = \begin{bmatrix} U & U & \cdots & U & 0 \end{bmatrix} \tag{11}$$

Combined with equations (9)~(11), the distribution of short-circuit turn currents in each layer of the Fe-based soft magnetic composite core reactor coil and the short-circuit turn currents under turn-to-turn short-circuit faults can be found.

When the reactor coil flows AC current, it is continuously subjected to electromagnetic force under the action of the alternating magnetic field, and the size of the electromagnetic force is proportional to the product of the magnetic induction strength and the flowing current, i.e., it is proportional to the square of the current. Then:

$$F \propto BI \propto I^2 \tag{12}$$

Assume that the Fe-based soft magnetic composite core reactor encapsulates the coil with the current flowing:

$$I = I_m \sin(2\pi ft + \varphi) \tag{13}$$

Then the electromagnetic force acting on the reactor envelope is:

$$F = AI^2 = AI_m^2 \left(\frac{1}{2} - \frac{1}{2}\cos(2\pi \cdot 2ft + 2\varphi) \right) \tag{14}$$

where A is the electromagnetic force coefficient.

2.2.2. Reactor vibration noise characteristics:

1) Effect of magnetostriction on core vibration noise. Magnetostriction is a macroscopic deformation of materials with ferromagnetic properties caused by changes in microscopic magnetic domains under the action of an external magnetic field. Specifically manifested as when the magnetic field of the reactor changes, the core silicon steel sheet in the direction of magnetization elongation or shortening phenomenon [25].

Assuming that the reactor has a supply voltage $U = U_{0sin\omega t}$, the electromagnetic induction strength of the core is $B = B_{0cos\omega t}$. Under the action of the magnetic field, the core undergoes microscopic magnetic domain changes to satisfy the relationship:

$$\frac{1}{L}\frac{\Delta L}{dH} = \frac{2\varepsilon_x}{H_c^2}|H| \tag{15}$$

Where L is the initial length, ΔL is the increment of the composite material under the action of the external magnetic field, $H = \frac{B}{\mu} = \frac{B}{B_S}H_C$ is the magnetic field strength, where μ is the core permeability, B_s is the saturation magnetic induction, H_c is the coercivity, and ε_x is the saturation flux coefficient of the silicon steel sheet.

Magnetostriction is generally described by the magnetostriction coefficient γ, viz:

$$\gamma = \frac{\square L}{L} = \frac{\varepsilon_x U_0^2}{2(NS\omega B_s)^2}(\cos 2\omega t + 1) \tag{16}$$

Where U_0 is the voltage amplitude, N is the number of turns of the winding, S is the cross-sectional area of the core.

The core vibration acceleration caused by magnetostriction is:

$$a = \frac{d^2(\Delta L)}{dt^2} = -\frac{2\varepsilon_x L U_0^2}{(NSB_s)^2}\cos 2\omega t \tag{17}$$

From the equation, it can be seen that the vibration frequency caused by magnetostriction of the core is 100 Hz.

The electromagnetic force on the core is another important cause of core vibration. Reactor magnetic field distribution along the core, mainly concentrated in the inner side of the yoke and the core cake and produce a large electromagnetic force, the presence of air gap between the core cake cushion block, so that the electromagnetic attraction between the adjacent core cake, resulting in core vibration.

2) Maxwell force on the core reactor vibration noise effects. Reactor core through the winding excitation, generating frequency and frequency consistent with the alternating magnetic field, in order to reduce the core column permeability, so that the impedance and the current is basically proportional to prevent the reactor in the work of magnetic saturation, the reactor core column exists by the non-conducting materials composed of the air gap, so the iron core between the cake with the change in the magnetic induction intensity produces an alternating electromagnetic force --- Maxwell force. -Maxwell force. In addition, silicon steel sheet stacked into the yoke in the magnetic flux density

changes in the presence of magnetostrictive effect, Maxwell force and magnetostrictive changes in the frequency are 2 times the frequency, that is, the main vibration frequency of the reactor. Reactor working flux density is low (usually less than 1.4T), magnetostriction is much lower than the vibration caused by the Maxwell force, so that the Maxwell force of the core cake is considered to be the main factor in the vibration of the reactor.

For transient magnetic fields defining the magnetic vector potential A, exists:

$$B = \nabla \times A = \mu H \tag{18}$$

where B is the magnetic flux density, μ is the magnetic permeability, and H is the magnetic field strength.

For a transient magnetic field with a winding excitation current density of J, the magnetic vector potential A can be solved from the following equation, which leads to the magnetic flux density B. i.e:

$$\nabla \times (\mu^{-1} \nabla \times A) + \sigma \frac{\partial A}{\partial t} = J \tag{19}$$

where σ is the conductivity.

The electromagnetic force between the core cake is the surface stress at the interface between the core air gap and the core cake manifold due to the magnetic field, which can be expressed by integrating the Maxwell stress tensor over the surface domain:

$$F = \int_{\Omega} \left(BH - \frac{1}{2} BHI \right) d\Omega \tag{20}$$

where Ω is the integration domain of the air gap and core cake interface, and I is the unit matrix.

Neglecting the core damping, the core vibration can be calculated from the vibration differential equation of the continuous multi-degree-of-freedom system.

where x is the displacement vector, M is the mass matrix of the core, and K is the stiffness matrix, which is related to the structural and material parameters of the core.

3. Optimized electromagnetic and noise design of core reactors

With the continuous improvement of voltage level and transmission capacity, the noise problem of Fe soft magnetic composite material core reactor becomes more and more serious, and although the external sound insulation measures have achieved a certain effect, they treat the symptoms but not the root cause, and bring about problems such as heat dissipation difficulties, affecting the appearance and infrared inspection, and so on. On the other hand, the previous research on core reactor mainly focuses on the vibration characteristics under industrial frequency excitation, and there is insufficient understanding of its vibration mechanism under multi-harmonic excitation in converter station, and the research on noise reduction measures for the equipment body lacks sufficient theoretical support. Therefore, in order to propose effective noise reduction measures, there is an urgent need to carry out research on the vibration generation mechanism and influencing factors of Fe soft magnetic composite core reactor, and optimize its parameters based on genetic algorithm, in order to further improve the stable operation of Fe soft magnetic composite core reactor.

3.1. Core reactor vibration noise modeling

3.1.1. Multi-physics field simulation module:

1) Magnetic Field Module for Iron Core Reactors. The analysis of the magnetic field problem for the Fe soft magnetic composite core reactor is based on Maxwell's system of equations. With the magnetic vector as the unknown quantity of the system of equations, other unknown quantities can be

calculated. The main dependent variable for the solution is the magnetic vector potential A, and it is possible to solve for variables such as the Lorentz force at each node, and the solution equation can be expressed as:

$$\sigma \frac{\partial A}{\partial t} + \nabla \times (\mu_0^{-1} \mu_r^{-1} \nabla \times A) = J_e \tag{21}$$

where μ_0 is the magnetic permeability of free space and μ_r is the relative magnetic permeability. where for the magnetic flux density B and the external current density $J_{\grave{o}}$ there is the following relationship:

$$\begin{cases} B = \mu_0 \mu, H = \nabla \times A \\ J_e = \dfrac{NI}{A} \end{cases} \tag{22}$$

Where, N is the number of coil turns, I is the winding current and A is the winding cross-sectional area.

2) Structural force field module of core reactor. In the structural force field simulation, the solid mechanics module of the finite element software is selected, and the structural force field solution domain equations can be expressed as follows:

$$m \frac{d^2 u}{dt^2} + \zeta \frac{du}{dt} + ku = F_V \tag{23}$$

where m is the mass matrix, ζ is the damping coefficient matrix, k is the stiffness matrix, and u is the displacement vector.

In order to describe the mechanical equations of the core, the linear elasticity equation is chosen to describe the magnetostriction, i.e:

$$\nabla \cdot \sigma = -F_V \tag{24}$$

where σ is the stress tensor and F_V is the volume force.

When a ferromagnetic material is located in a magnetic field, the magnetic field within the material will change, and when stabilized, it will show a significant enhancement of the potential, which makes the ferromagnetic material show a strong magnetism in the external magnetic field, a phenomenon known as the magnetization of ferromagnetic materials. This phenomenon is called the magnetization of ferromagnetic materials. The reason why ferromagnetic materials can be magnetized is that there are many very small natural magnetization areas called magnetic domains, each of which can be regarded as a micro-magnet. When the ferromagnetic material applied to the external magnetic field, the direction of its magnetization changes, after stabilization of the internal magnetic domains and the magnetic field in the same direction.

3) Core reactor sound field module. The pressure sound field module is selected in the sound field analysis, and the variable solved by the pressure production field module is the sound pressure p. The solved domain sound pressure fluctuation equation is:

$$-\frac{1}{c^2} \frac{\partial^2 p}{\partial t^2} + \nabla^2 p = 0 \tag{25}$$

where c is the speed of sound and p is the sound pressure.

The relationship between sound pressure and sound velocity can be described by applying the linear equation of motion as:

$$\rho_0 \frac{\partial u}{\partial t} = -\nabla p \tag{26}$$

where ρ_0 is the air density.

The vibration noise of Fe-based soft magnetic composite core reactor in finite element analysis is essentially a multi-physics field coupling study, which involves the coupling between electromagnetic field, structural force field and acoustic field. The so-called coupling, physics refers to two or more systems or two forms of motion through a variety of interactions and influence each other to the joint phenomenon. In electronics it refers to the transfer of energy from one circuit part to another. In short, the coupling involved in the study of the object must be two or more than two, and in the study of the object, according to the coupling with or without coupling elements can be divided into direct coupling and indirect coupling, and according to the direction of the coupling can be divided into one-way coupling and two-way coupling.

3.1.2. Finite element simulation modeling. In this paper, the Fe-based soft magnetic composite core reactor of model CKSC-105/20 is taken as an object and its three-dimensional multi-physics field simulation model is constructed as shown in Fig. 1. The reactor has a rated capacity of 10 kVA, a nominal system voltage of 12 kV, a rated operating current of 110 A, and a rated reactance of 3 Ω. The reactor windings are made of multilayered flat copper wires and cast with epoxy resin, with two layers in each phase, a single-layer coil with a turn count of 90, and a single-layered coil with a width of 18.8 mm. The upper and lower yokes of the core are made of oriented Fe-based soft magnetic composites. The upper and lower yokes of the core are made of oriented Fe-based soft magnetic composites, while the core column consists of multiple core cakes stacked on top of each other and separated by epoxy cloth panels to form an air gap.

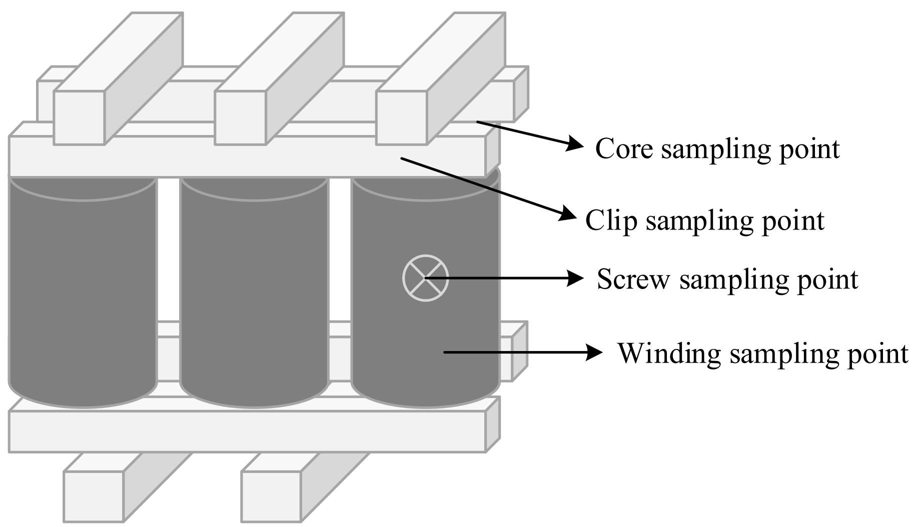

Fig. 1. 3D simulation model of Fe base soft core reactor

Considering the vibration amplitude and the difficulty of detection, this paper selects sampling points on each group of components of the core reactor to facilitate the subsequent comparison of simulation and test results. The model focuses on the influence of the screw used to fasten the upper yoke, the lower yoke and the screw running through the double-layer winding, as well as its end bolts, support pads and other structural components. On the one hand, the vibration of the yoke along the y-direction is limited to a certain extent by the clamps on its left and right sides, top and bottom, while the vibration amplitude of the winding along the z-direction is influenced by the pads and clamps on its top and bottom. On the other hand, the mutual influence of the vibration of the core and the winding can also be transmitted through the structure of the clamps, pads, and threading screws, thus realizing the vibration analysis of the reactor under the joint action of multiple forces.

3.1.3. Parameter setting and boundary conditions. According to the vibration and noise characteristics of the Fe-based soft magnetic composite core reactor described in the previous paper, combined with the finite element method, the magnetic-structural-acoustic multi-field coupling model of the Fe-based soft magnetic composite core reactor is established by using the finite element simulation software to calculate and analyze the magnetic, structural, and acoustic fields during its operation.

In the simulation calculation, in order to make the model calculation results more in line with the actual equipment, on the basis of the accurate characterization of the reactor core structure, in order to improve the calculation efficiency of the model to make the following settings:

1) Because the vibration of the reactor core can be calculated without considering the heat dissipation of the core, the marble cushion in the structure of the air gap between the core cake is equivalent to a piece.

2) Set the lower surface of the iron yoke as a fixed constraint to simplify the fixed structure of the external box.

3) Simplify the bolts and connectors to be uniformly added to the core column in the form of loads.

4) Include the main parts such as the core, windings, yoke, magnetic splitter, and tank, and set the core as a magnetostrictive material in order to calculate the magnetostrictive force applied to the core, and apply Maxwell's force as a load on the surface of the core structure. In addition, the internal space of the Fe-based soft magnetic composite core reactor tank is set as the transformer oil in the simulation, and the components in the tank are surrounded by this domain.

Table 1 shows the simulation parameters of the Fe-based soft magnetic composite core reactor. The specific steps of the calculation process are:

Step1 Calculate the magnetic field generated by the winding excitation.

Step2 Couple the calculated Maxwell force and magnetostrictive force as loads into the structural field.

Step3 Calculate the vibration parameters such as core force, vibration displacement, acceleration, etc. in the structural field.

Step4 Perform the Fast Fourier Transform (FFT) of the stresses to obtain the corresponding frequencies and amplitudes.

Step5 Take the stress as the noise source of the sound field, and solve to get the sound field parameters such as sound pressure level around the reactor, sound power level and sound pressure level in the external field.

Table 1. Simulation parameters for Fe base soft magnetic Iron core reactor

Parameters	Value	Code
Stress (MPa)	0	X1
Air gap number (Per)	16	X2
Gap height (mm)	9	X3
Core diameter (mm)	400	X4
Core distance (mm)	100	X5
Iron cake height (mm)	50	X6
Iron yoke height (mm)	350	X7
Vibration displacement (μm)	25	X8
Core mass (kg)	9279.16	X9
Core loss (W)	1753.48	X10
Reactance (Ω)	120.54	X11

3.2. Parameter optimization based on genetic algorithm

3.2.1. Mathematical description of genetic algorithms. Genetic Algorithm (GA), as an intelligent algorithm for global search and optimization based on the mechanism of biological hereditary evolution, uses genetic operators to mimic the hereditary characteristics of organisms by completing the search for the optimal solution with the mechanisms of selection, crossover, and mutation in the hereditary and evolution of organisms. The traditional solution to the optimization problem mainly consists of two categories: numerical method and analytical method, but due to the complexity of the problem becomes larger, the traditional solution method can not solve the problem well, while the genetic algorithm solution is not subject to the specific problem constraints, and can be solved complex problems, which provides a new solution idea for solving these problems [26].

Genetic algorithms are in various forms and are mainly composed of the following four points:

1) Determining the representation of variables. Encoding is the process of representing each possible point in the search space of the problem as a feature string of definite length. The feature string is the individual or chromosome, and the individual is represented by a string, and when coding a multivariate problem, a variable corresponds to a component of the entire string, which is also known as a gene or genetic factor, and all the individuals make up the population.

2) Determining the fitness function. The fitness is a measure used to distinguish the degree of superiority of the survival of the population, the fitness is calculated by the fitness function, the algorithm in the search of evolution is only based on the fitness function and the fitness value of each individual to carry out the search. Therefore, the fitness function is related to whether the algorithm can quickly and accurately complete the search for the optimal solution. The fitness function generally has the following two ways:

If the objective function is a maximum value solution problem, there are:

$$F(x)=\begin{cases} C_{\max}+f(x), f(x)<C_{\max} \\ 0, \text{other} \end{cases} \tag{27}$$

where $C_{\max}$ is the maximum estimate of the objective function $f(x)$, $f(x)$ is the objective function, and $F(x)$ is the fitness function.

If the objective function is a minimum value solution problem, there is:

$$F(x)=\begin{cases} f(x)-C_{\min}, \text{when}\, f(x)>C_{\min} \\ 0, \text{other} \end{cases} \tag{28}$$

Where, $C_{\min}$ is the maximum estimate of the objective function $f(x)$, $f(x)$ is the objective function and $F(x)$ is the fitness function.

3) Determining the genetic operators of the algorithm. The simulation of the eugenic and hereditary processes of biological evolution in genetic algorithms is accomplished through three basic operational operators, namely selection, crossover, and mutation. The magnitude of the likelihood of offspring retention is determined by calculating the probability of each individual's fitness. If an individual i, whose fitness is f_i, the probability of its selection is expressed as:

$$p_i = \frac{f_i}{\sum_{i=1}^{u} f_i} (i = 1, 2, \ldots\ldots, u) \tag{29}$$

where p_i is the probability of an individual being selected, u is the size of the population, and f is the fitness of the individual.

4) Determine the criterion to stop running. The convergence of the genetic algorithm is heuristic, there is no strict convergence criterion, the current commonly used basis for judging convergence is to determine whether the algorithm has reached convergence by whether the number of calculations reaches the maximum number of iterations, and whether the optimal solution has no change within a certain time number of conditions.

3.2.2. System optimization modeling. Considering the many optimization parameters of the Fe-based soft magnetic composite core reactor, while reducing the complexity of the optimization search process, the design variables of the different physical field systems are stratified using the sensitivity analysis method. The design variables with higher sensitivity of each physical field are taken as the independent variables for the optimization of the subsystem, and the design variables with low sensitivity are treated as the system-level design variables. The independent design variables within the subsystems are only optimized in this system, and the system-level design variables are transferred to the subsystems by the system-level optimization.

In accordance with the idea of collaborative optimization, the optimization model of Fe-based soft magnetic composite core reactor is established as:

$$\begin{cases} \min \quad M_r = f(w_b, w_e, g, n, w_{i,c}, w_{t,c}, w_{s,t}, d, H_c, W_c) \\ s.t. \quad \sum_{i=1}^{n^{elec}} (X_i - X_i^{elec})^2 + \sum_{i=1}^{n^{elec}} (Y_i - Y_i^{elec})^2 \le \varepsilon \\ \quad \sum_{i=1}^{n^{temp}} (X_i - X_i^{temp})^2 + \sum_{i=1}^{n^{temp}} (Y_i - Y_i^{temp})^2 \le \varepsilon \\ \quad \sum_{i=1}^{n^{struct}} (X_i - X_i^{struct})^2 + \sum_{i=1}^{n^{struct}} (Y_i - Y_i^{struct})^2 \le \varepsilon \\ \quad (X, Y)^T_{\min} \le (X, Y)^T \le (X, Y)^T_{\max} \end{cases} \tag{30}$$

where M_r is the amount of metal conductor used in the Fe-based soft magnetic composite core reactor, and $X_i^{elec}, X_i^{temp}, Y_i^{elec}, Y_i^{temp}, Y_i^{struct}$ are the system variables and independent variables of the electromagnetic, structural, and noise systems, respectively, where the sum of squares of the differences between the system variables and the optimal solutions of the subsystems is less than a minuscule value ε.

3.2.3. Model optimization solution process. In this paper, GA algorithm is used to solve the multi-parameters in the vibration noise optimization model of Fe-based soft magnetic composite core reactor established in the previous paper. In order to accurately evaluate the accuracy of the optimization algorithm, this paper adopts the root-mean-square error as the error between the model calculation value and the experimental measurement value, so as to convert the problem of extracting the parameters of the model into the optimization problem of the minimum value of the objective function. Figure 2 shows the specific flow of GA algorithm to solve the vibration noise optimization model of Fe-based soft magnetic composite core reactor.

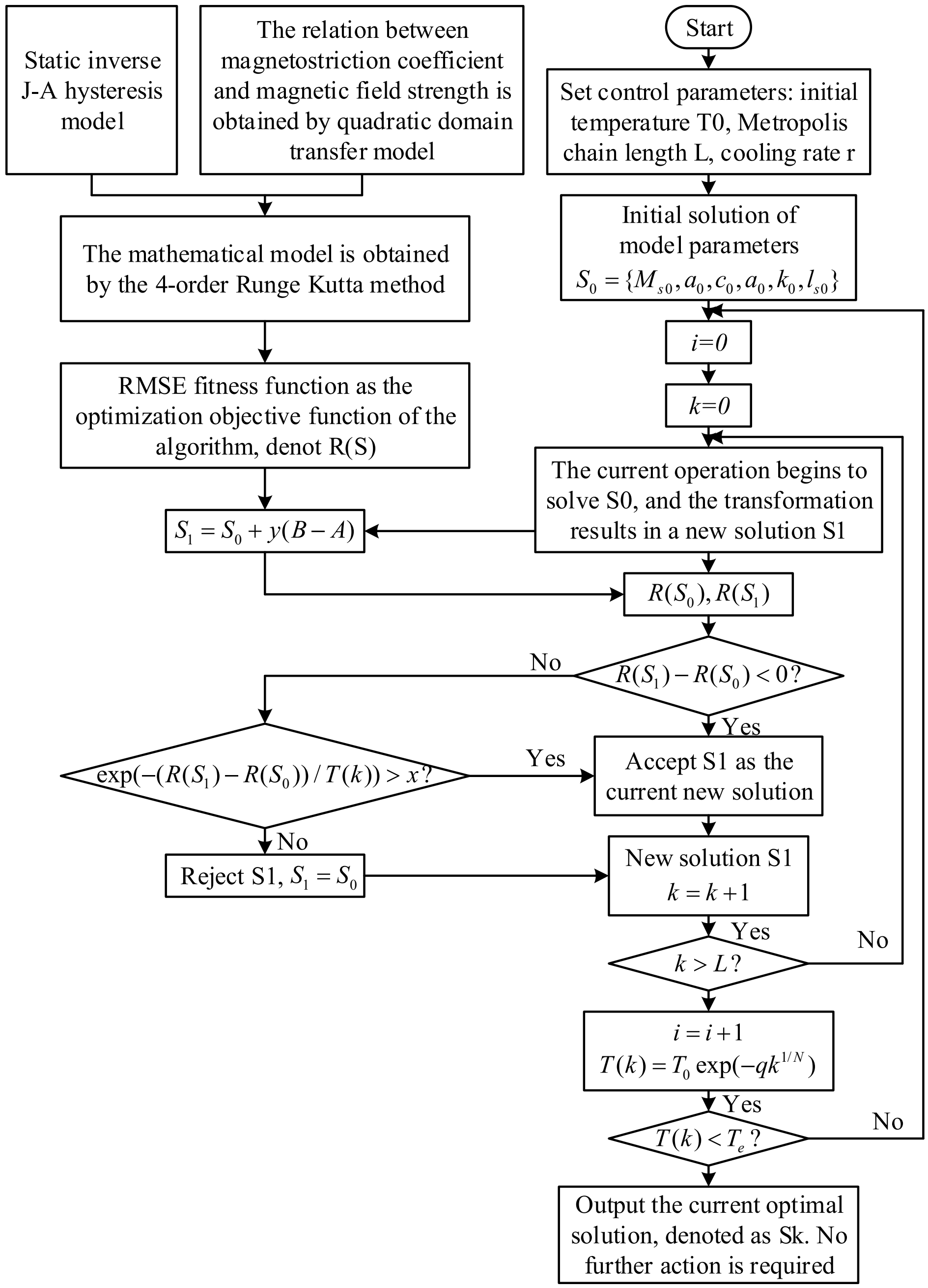

Fig. 2. The solution process of GA algorithm

The steps are as follows:

1) Set the parameters of the input algorithm initial, temperature t_0, Metropolis chain length, random initial value S_0, cooling rate r, number of iterations $k=0$.

2) Generate a new state value S_i, calculated as:

$$S_1=S_0+y(B-A) \tag{31}$$

where y is a random perturbation that satisfies a uniform distribution, and B, A is the upper and lower bounds of the design variables, respectively.

3) Metropolis criterion. Substitute S_1 into the magnetostrictive model equation to calculate the root-mean-square error function, and the result is denoted as $R(S)$. When the increment between the new solution S_1 and the current solution S_0 is less than 0, the new solution is accepted, and vice versa when it is greater than 0, the decision of whether or not to accept the new solution is based on the probability P, and the probability P is computed by the formula:

$$P = e^{-\frac{R(S_1)-R(S_0)}{T(k)}} \tag{32}$$

If $P \geq random[0,1]$, the new solution S_1 is accepted, otherwise the current solution is kept.

4) Crossover Variation. Loop through steps (2) to (3) in the iteration process to get the optimal solution at one temperature. Then:

$$T(k) = T_{0,j} e^{(-qk^{\frac{1}{N_1}})} \tag{33}$$

Where $T_{0,j}$ is the current solution and N_1 is the number of design variables. When the solution is smaller than the set iteration condition, the iteration is completed to output the optimal solution.

4. Validation of electromagnetic and noise optimization of core reactors

Power transformer as a key equipment in the process of power generation, transmission and distribution in the electric power industry, its safe, stable and reliable operation is crucial. Among them, Fe-based soft magnetic composite iron core reactor plays a crucial role in the electromagnetic performance and mechanical strength of the transformer, and the failure caused by the core problem occupies a large proportion in the total transformer failure. Therefore, it is necessary to assess the condition of the core reactor and optimize the structure of the Fe-based soft magnetic composite core reactor to enhance the application life of the power transformer.

4.1. Simulation analysis of core reactor performance

4.1.1. Magnetic field variation in core reactors. Based on the finite element model of Fe-based soft magnetic composite core reactor constructed in the previous section, a harmonic effect is given to this core reactor in the VC platform, and combined with the magnetostrictive equation, it is known that the magnetic induction strength of the core reactor will show different trends under the harmonic effect. Figure 3 shows the trend of the magnetic induction strength of the core reactor with time after the superposition of the 6th harmonic with a harmonic content of 20% and a phase difference of 30° from the fundamental wave with the action of the fundamental wave. Due to the application of three-phase symmetrical harmonic excitation, the three-phase cores have similar flux density distribution laws, and the magnetic density fluctuations of the three-phase core reactors are all in the range of 0.01T to 1.24T. Therefore, the maximum value of the magnetic density period of the A-phase core is taken as the output of the batch simulation.

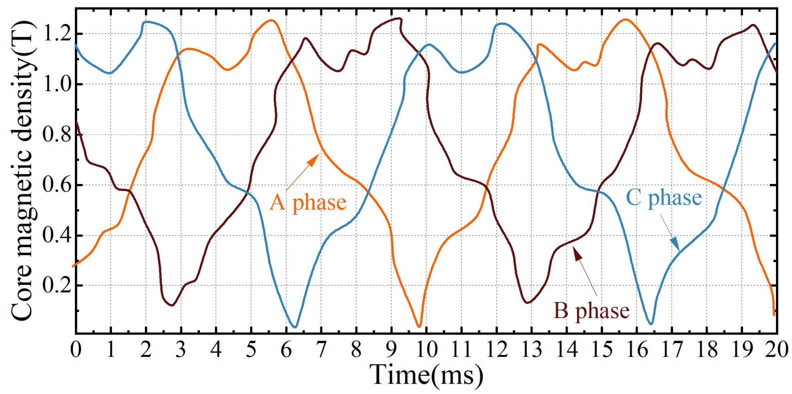

Fig. 3. The curve of the iron core magnetic flux

The harmonic excitation parameters are set using the visual batch processing interface developed based on the VC platform, and a total of 150 3D nonlinear transient magnetic field simulations are carried out over a period of 5 h. Since the magnetic density distribution is symmetric about φ=180° within 0~360°, the curve is taken within 0~180°, and the simulation results of the magnetic field variations of the core reactor are shown in Fig. 4. Among them, Fig. 4(a)~(c) shows the variation of 2nd, 4th and 6th harmonic magnetic induction intensity with harmonic phase angle and content, respectively.

The magnetic density maxima of the 2nd and 6th harmonics have a distribution law that increases with the increase of the harmonic phase angle within 0~180° when the harmonic content is the same, and the opposite is true for the 4th harmonic.The 4th and 6th harmonic magnetic densities increase with the increase of the harmonic content when the harmonic phase angle is the same, while the 2nd harmonic exhibits a different distribution law that decreases with the increase of harmonic content when the harmonic phase angle is small, and decreases with the increase of harmonic content when the harmonics phase angle is close to 180°, and increases with the increase of harmonic content when the harmonics phase angle is close to 180°. When the phase angle is close to 180°, the maximum value of magnetic density increases with the increase of harmonic content, and the turning point is located near the 2nd harmonic phase angle of 54°, which corresponds to the maximum value of magnetic density in phase A of 1.183T, which is similar to the maximum value of magnetic density of the core in phase A under the action of fundamental wave, with a difference of only 4.82%. Therefore, there are more obvious changes in the magnetic induction strength of Fe-based soft magnetic composite core reactors under different harmonic effects, which is of some significance for grasping the distribution law of magnetic induction strength of core reactors under harmonic effects.

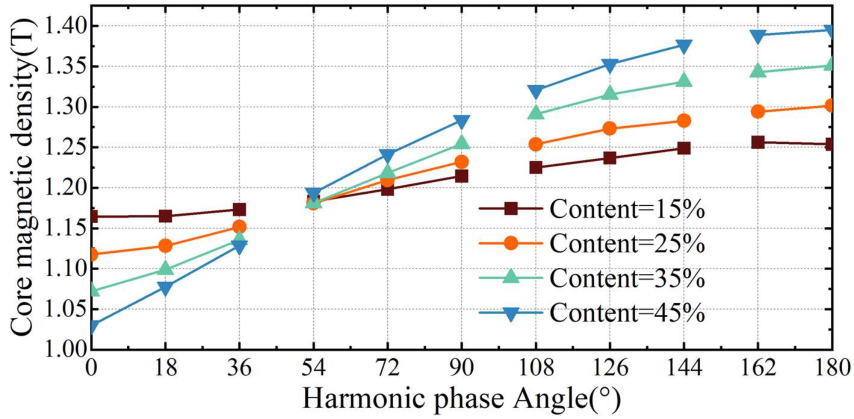

(a) Two harmonic magnetic induction intensities

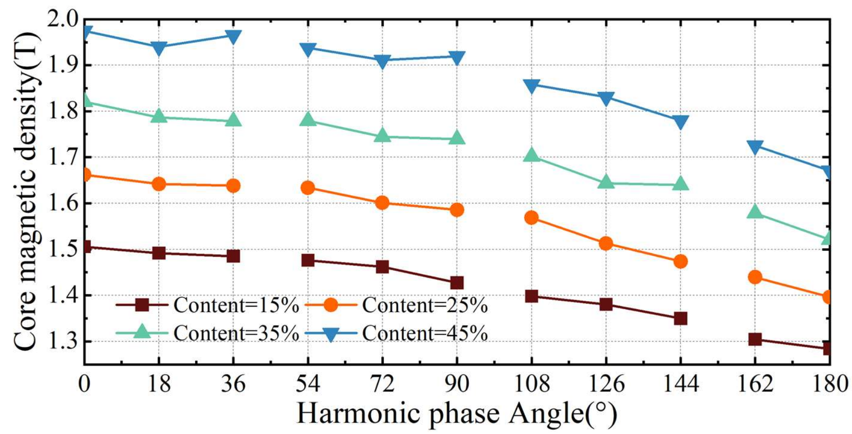

(b) Four harmonic magnetic induction intensities

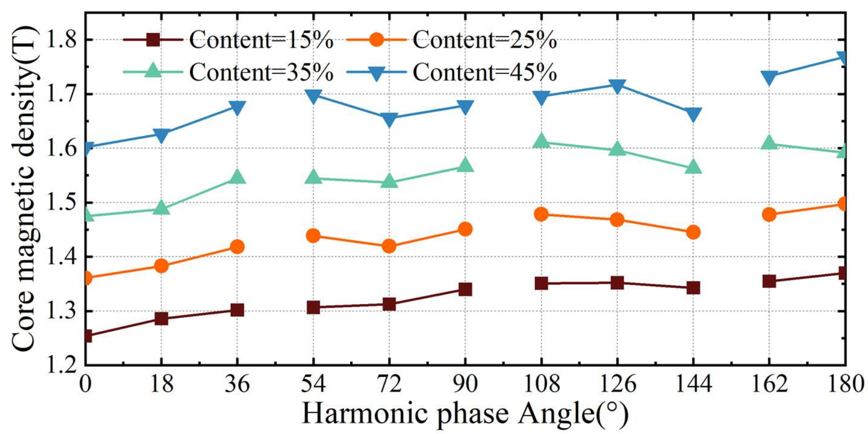

(c) Six harmonic magnetic induction intensities

Fig. 4. Simulation results of magnetic field change

4.1.2. Core vibration signal characteristics. For the core reactor, its vibration change affects the operation effect of the reactor to a certain extent, and the change of the fastening state of the core in the Fe-based soft magnetic composite core reactor will have a greater impact on its vibration state and be reflected in the vibration signal on its surface. Therefore, the limit state of completely loosened clamps on the core is used as a comparison to explore the significant change characteristics of vibration signals before and after the core is loosened.

In the low voltage side of the core reactor voltage to 400V, when the transformer core flux is close to the rated operating state, measured when the core is tightened and the upper clamps completely loosened B-phase measurement point in the time domain vibration signal waveforms in the three frequency cycles as shown in Figure 5. Figure 5(a)~(b) shows the vibration signals of the fastened and loosened core, respectively. In the figure, the vibration signals in the core tightening and loosening state show a periodicity of 100 Hz as a whole, but due to the vibration signals containing certain high harmonic components, resulting in certain distortion in the time domain waveform of the vibration signals. Loosening of the clips of the Fe-based soft magnetic composite core reactor leads to a decrease in the binding force on the core and an enhancement of the vibration, and the comparison shows that the peak value of the vibration signal increases from 2.41 V to 3.79 V after the loosening of the core. At different core states, the core vibration signal score increases significantly.

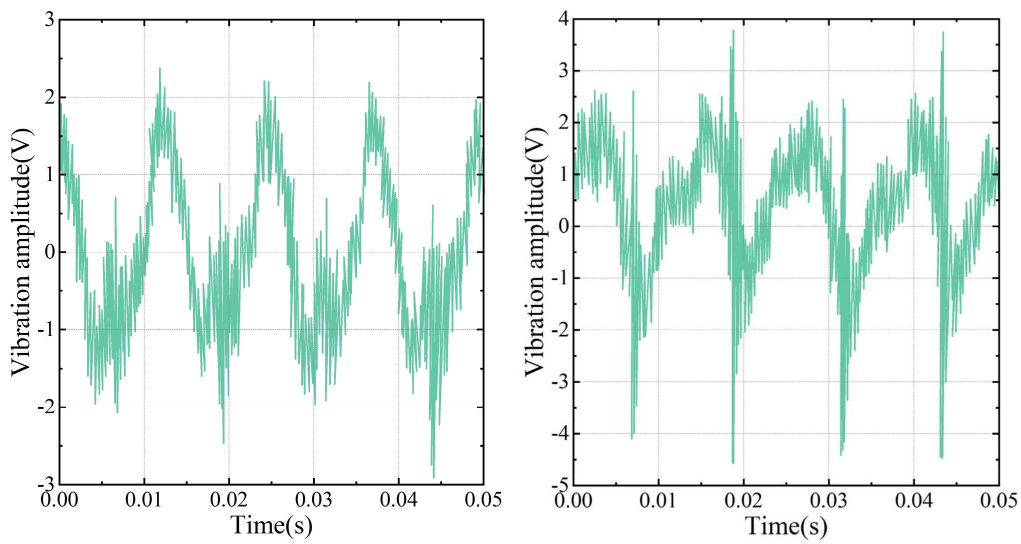

(a) Iron tight (b) Loose core

Fig. 5. The vibration of the iron heart is loose and the vibration signals

The frequency domain distribution of the vibration signal within 0~1200Hz before and after the core loosening is compared, and the comparison results are shown in Figure 6. In the figure, the harmonics in the state of core tightening are mainly the higher octave components of 100Hz, and the frequency components of the vibration signal are mainly concentrated in 500Hz and below, with the components above 500Hz accounting for a relatively small amount. Among them, the amplitude of the 100Hz harmonic component is larger, thus leading to the vibration signal time-domain waveform in Fig. 5(a) to appear asymmetric waveforms in half a cycle.

Due to the increase of the core vibration intensity caused by the loosening of the core clamps, the amplitudes of the 100, 250, and 700 Hz frequency components of the vibration signal increase in Fig. 6. Among them, the amplitude change of 250 and 700Hz components is more obvious, probably due to the change of the mechanical structure of the core so that the intrinsic frequency of the transformer vibration has changed, close to the intrinsic frequency of the transformer exists at 250Hz and 450Hz, so that the vibration at this place is enhanced.

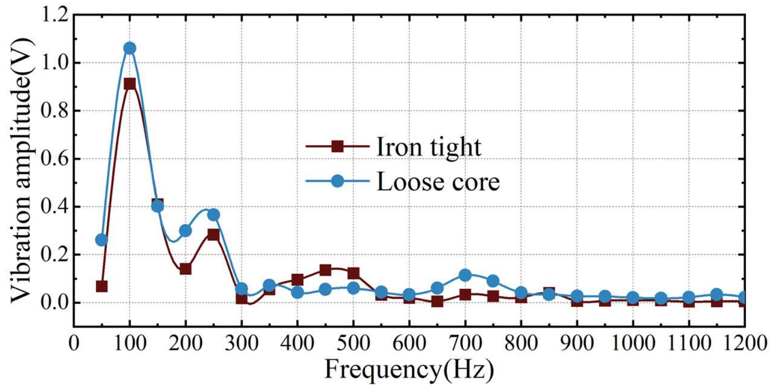

Fig. 6. Frequency distribution of vibration signal

In addition, in order to further verify the vibration displacement of the Fe-based soft magnetic composite iron core reactor under harmonic action, based on the existing studies, the contribution of magnetostrictive force to the vibration displacement of the reactor is much smaller than that of Maxwell force to the vibration displacement of the reactor core. Therefore, the vibration displacement induced by Maxwell force under the fundamental wave condition can be used to characterize the vibration displacement of Fe-based soft magnetic composite core reactor. The silicon steel core reactor is chosen as a comparison, and its vibration displacement comparison with the Fe-based soft magnetic composite iron core reactor is shown in Fig. 7.

From the figure, it can be seen that the core vibration displacement of the Fe-based soft magnetic composite iron core reactor is much smaller than that of the conventional silicon steel core reactor. The maximum displacement of the silicon steel series reactor reaches 5.17*10-5m, while the maximum displacement of the Fe-based soft magnetic composite core reactor is only 0.25*10-5m. Compared with the two, the vibration displacement of the measurement point of the Fe-based soft magnetic composite core reactor is reduced by 95.16% compared with the vibration displacement of the measurement point of the silicon steel reactor core. The feasibility of applying Fe-based soft magnetic composites in the structural design of the core reactor is fully demonstrated, which can greatly reduce the vibration displacement of the core surface during the operation of the core reactor.

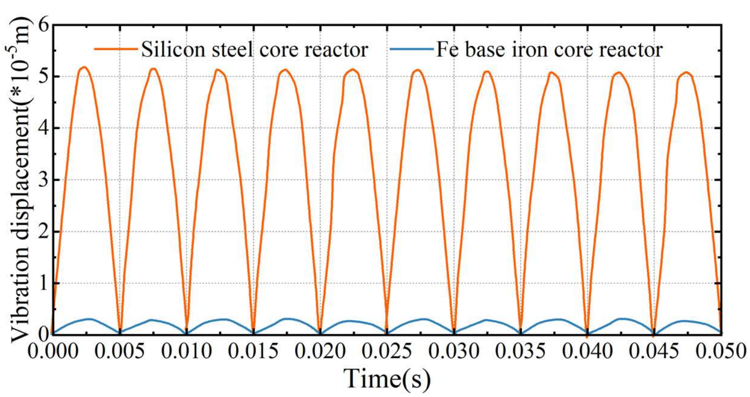

Fig. 7. Vibration displacement contrast of iron core reactor

4.1.3. Core Vibration Sound Pattern Characteristics. The voltage waveform added in this experiment contains two pulses, which simulate the opening and closing process of the single valve in the actual operation of the saturated reactor, respectively. In these two processes, the voltage amplitude and voltage change rate are the largest, so that the Fe-based soft magnetic composite iron core reactor is sufficiently magnetized to produce the strongest magnetostrictive effect, which can better reflect the actual vibration characteristics of the iron core. Through the Fourier transform, the voltage harmonic distribution of the Fe-based soft magnetic composite iron core reactor under different charging voltages is obtained as shown in Figure 8.

The voltage of the Fe-based soft magnetic composite core reactor contains a large number of harmonic components, and the odd and even harmonics account for a comparable proportion, and are less affected by the change of voltage amplitude. The frequency spectrum from 0 to 30 kHz is divided into 10 bands with every 3 kHz as a band, and the percentage of different bands is calculated respectively. With the increasing voltage amplitude, the proportion of 0~6kHz gradually decreases. When the charging voltage reaches 2.5kV, the proportion is 35.12%, which is about 16% lower than that of 0.1kV, but it is still the main component of harmonics. The proportion of 6-30kHz fluctuates, and the overall tendency is to increase. Among them, the harmonic components of charging voltage 0.5kV and 0.6kV change most obviously. Further analysis of the voltage waveform found that the charging voltage of 0.6kV voltage waveform has a sudden drop, continue to boost the voltage harmonic component change trend slows down.

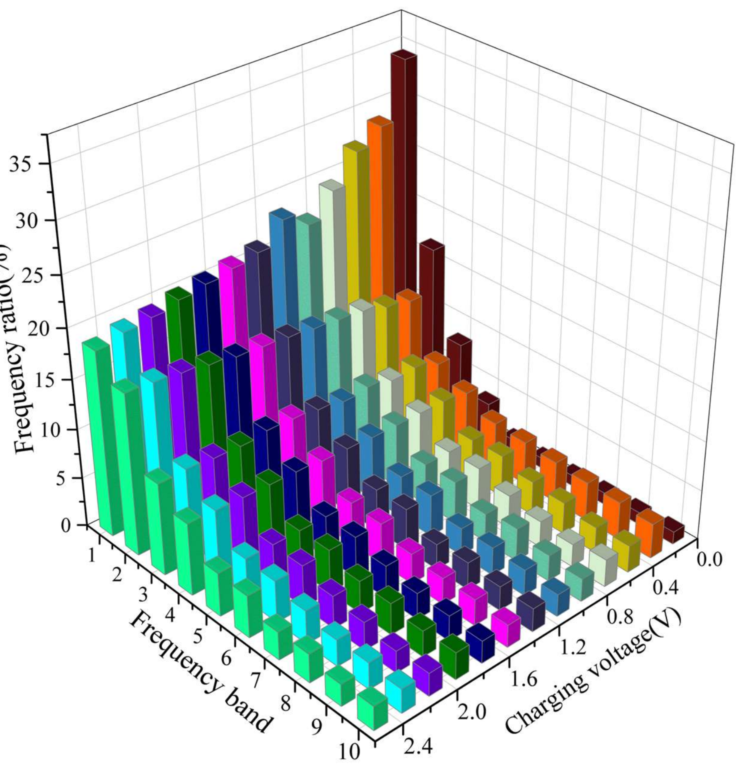

Fig. 8. Voltage harmonic distribution of iron core reactor

In order to study the variation of vibration sound produced by the Fe-based soft magnetic composite reactor core with increasing voltage, the amplitude of the time-domain acoustic signals at four measurement points is plotted on a box-and-line diagram as shown in Fig. 9. The upper and lower edges of the graph are 1.5 times the standard deviation of the data. As can be seen from the figure, the trend of sound changes at different measurement points is roughly the same, at a voltage of 0.3kV, the amplitude of all the measurement points is below 0.2V, at which time the core of the Fe-based soft magnetic composite reactor is in a saturated state, generating a large vibration noise. As the voltage increases, the core magnetic unsaturation and magnetic saturation state conversion accelerated, resulting in high-frequency components of the vibration noise increased significantly, of which the measurement point 3 by the voltage growth of the impact of the larger, acoustic signal amplitude change of more than 3.5 times. However, Fe-based soft magnetic composite material reactor core reactor vibration and voltage amplitude quadratic nonlinear relationship, when the voltage amplitude reaches 1.3kV, the acoustic signal amplitude growth rate decreases, and gradually tends to level off.

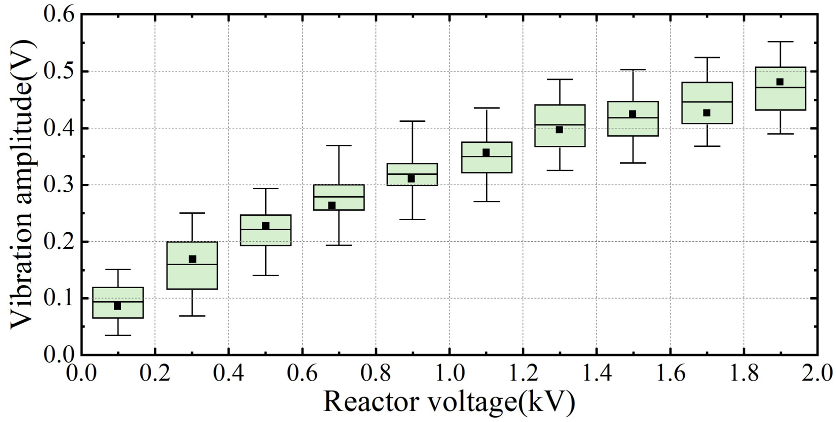

Fig. 9. The amplitude of the vibration signal changes

4.2. Validation of core reactor model optimization

4.2.1. Sensitivity of structural parameters. According to the structural characteristics of Fe-based soft magnetic composite iron core reactor, combined with the reactor parameters given in the previous paper, the structural parameters that may affect the reactor performance objectives are initially screened as design variables. And based on the optimization model of Fe-based soft magnetic composite core reactor constructed in this paper, it involves many parameters. In order to improve the optimization efficiency, this paper adopts sensitivity analysis to study the influence law of structural parameters on each physical field characteristic index of the reactor. According to the degree of correlation, the parameters with higher degree of correlation are selected for the next step of optimization, so as to realize the parameter dimensionality reduction in the optimal design of Fe-based soft magnetic composite iron core reactor.

The degree of influence of each system design variable of Fe-based soft magnetic composite material iron core reactor on each physical field characteristic index, i.e., sensitivity, the greater the sensitivity, the greater the degree of influence on the state variables. Based on the sample data, the response relationship between the design parameters and the state variables is established so as to obtain the normalized sensitivity results as shown in Fig. 10.

From the figure, it can be seen that for the electromagnetic field of the Fe-based soft magnetic composite core reactor, the stress (X1) has a significant effect on the inductance value, and its normalized sensitivity reaches 0.468, and the distribution of the air gap changes the distribution of the internal flux magnetic circuit of the core reactor, which in turn changes the size of the main inductance and leakage inductance. The core diameter (X4) also has a certain effect on the inductance size, the core diameter increases, the main flux magnetic circuit area increases accordingly, resulting in an increase in the main inductance. The noise field is mainly affected by the number of air gaps (X2) and the height of the air gap (X3), and the rest of the structural parameters also have a certain effect on the noise field distribution. The influence of different structural parameters on the vibration displacement of Fe-based soft magnetic composite core reactor is more complicated, and the influence of stress (X1) is the most significant. In order to simplify the optimization process, an agent modeling technique is used to construct a response model between structural parameters and different physical fields, which provides support for optimizing the structural parameters of the Fe-based soft magnetic composite iron core reactor.

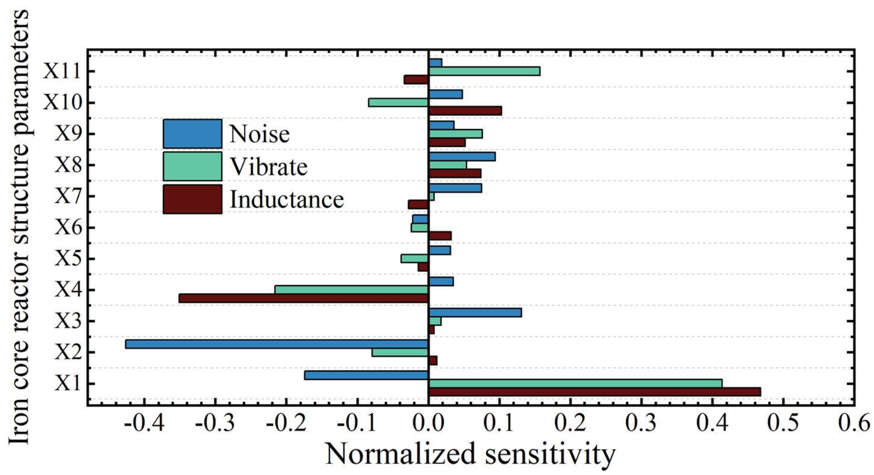

Fig. 10. Sensitivity of structural parameters

4.2.2. Optimization results of structural parameters. In order to verify the specific effect of the optimization model of Fe-based soft magnetic composite core reactor solved by GA algorithm in this paper, RSM and Kriging are chosen as the comparison algorithms to optimize and solve the structural parameters of the Fe-based soft magnetic composite core reactor, and the optimization results of the structural parameters of different methods are shown in Table 2.

Table 2 shows the optimization results of the structural parameters of different methods. As can be seen from the table, RSM algorithm, Kriging algorithm and GA algorithm proposed in this paper effectively reduce the vibration of the core while meeting the electrical performance conditions of the Fe-based soft magnetic composite core reactor, among which, GA algorithm has the best optimization effect of vibration damping and reduces the electromagnetic loss of the core by 13.83% and 4.65% compared to the RSM algorithm and the Kriging algorithm, respectively. At the same time, the metal usage of the core is reduced by 15.27% compared to the initial parameters. In addition, in order to verify that the optimization scheme proposed in this paper is effective, the magnetic field distribution and vibration displacement distribution of the Fe-based soft magnetic composite core reactor are analyzed by electromagnetic field-structure force field simulation based on the parameters in the table. It is found that, compared with the simulation results of the initial structure, the magnetic density distribution of the core remains basically unchanged under the three optimization schemes, and the magnetic field reactance values of the three optimization methods are 116.84 Ω, 113.92 Ω, and 110.67 Ω, with the errors of 3.07%, 5.49%, and 8.19%, respectively, compared with the actual values, and the optimization of the GA algorithm has the largest magnitude and meets the requirements of electromagnetic performance parameters . Compared with the simulation results of the initial structure, the vibration displacements of the core under the three optimization schemes have large changes, and the optimized vibration displacements are mainly concentrated at the core cake, and the maximum vibration displacements of the core under the three optimization methods are 23.8 μm, 22.6 μm, and 20.5 μm, respectively, of which the smallest vibration displacement is obtained by the GA algorithm. In conclusion, the optimization of the structure-related parameters of Fe-based soft magnetic composite core reactor using genetic algorithm can significantly reduce the vibration displacement of the core reactor.

Table 2. The structural parameters of different methods are optimized

Parameter	Initial	RSM	Kriging	GA
X1	0	0.25	0.28	0.32
X2	16	14	15	18
X3	9	9.16	8.24	7.93
X4	400	400	400	400
X5	100	100	100	100
X6	50	45	45	40
X7	350	330	330	330
X8	25	23.8	22.6	20.5
X9	9279.16	8524.93	9053.28	9137.46
X10	1753.48	1579.75	1427.69	1361.32
X11	120.54	116.84	113.92	110.67

5. Conclusion

Based on the magnetostrictive force and Maxwell force, the vibration and noise characteristic equations of Fe-based soft magnetic composite core reactor are established, and the multi-physics simulation model of Fe-based soft magnetic composite core reactor is constructed by combining the electromagnetic field-structural force field-acoustic field. The structural parameter optimization model of Fe-based soft magnetic composite core reactor is designed, and the model is solved by genetic algorithm to obtain the optimal core reactor parameters. It is found that the peak value of the vibration signal of the core reactor increases from 2.41 V to 3.79 V after the clamps of the core reactor are loosened, and the maximum displacement of the Fe-based soft magnetic composite core reactor is only 0.25*10-5m. The GA algorithm has the best optimization effect for vibration damping, and the electromagnetic loss of Fe-based soft magnetic composite core reactor is reduced by 13.83% and 4.65% compared to RSM algorithm and Kriging algorithm, respectively. Therefore, the use of genetic algorithm can effectively optimize the electromagnetic and noise structure design of Fe-based soft magnetic composite core reactor, which can provide a guarantee for expanding the application path of Fe-based soft magnetic composite materials and enhancing the application life of core reactor.

Funding

This work was supported by State Grid Hebei Electric Power Co., LTD. Science and Technology Project funding: A new type of low noise core reactor based on Fe based soft magnetic composite material is developed (5204CZ240002).

References

[1] Wang, Y., Guo, C. H., Chen, X. J., Jia, L. Q., Guo, X. N., Chen, R. S., ... & Wang, H. D. (2021). Carbon peak and carbon neutrality in China: Goals, implementation path and prospects. China Geology, 4(4), 720-746.

[2] Liu, L., Wang, X., & Wang, Z. (2023). Recent progress and emerging strategies for carbon peak and carbon neutrality in China. Greenhouse Gases: Science and Technology, 13(5), 732-759.

[3] Rodrigues, E. M., Godina, R., & Pouresmaeil, E. (2020). Industrial applications of power electronics. Electronics, 9(9), 1534.

[4] Scirè, D., Lullo, G., & Vitale, G. (2022). Non-linear inductor models comparison for switched-mode power supplies applications. Electronics, 11(15), 2472.

[5] Thivagar, M. L., Ahmed, M. A., Ramesh, V., & Hamad, A. A. (2020). Impact of non-linear electronic circuits and switch of chaotic dynamics. Periodicals of Engineering and Natural Sciences (PEN), 7(4), 2070-2091.

[6] Maza-Ortega, J. M., Acha, E., García, S., & Gómez-Expósito, A. (2017). Overview of power electronics technology and applications in power generation transmission and distribution. Journal of Modern Power Systems and Clean Energy, 5(4), 499-514.

[7] Liang, X., & Andalib-Bin-Karim, C. (2018). Harmonics and mitigation techniques through advanced control in grid-connected renewable energy sources: A review. IEEE Transactions on Industry Applications, 54(4), 3100-3111.

[8] Hu, Z., Han, Y., Zalhaf, A. S., Zhou, S., Zhao, E., & Yang, P. (2023). Harmonic sources modeling and characterization in modern power systems: A comprehensive overview. Electric Power Systems Research, 218, 109234.

[9] Ghorbani, M. J., & Mokhtari, H. (2015). Impact of Harmonics on Power Quality and Losses in Power Distribution Systems. International Journal of Electrical & Computer Engineering (2088-8708), 5(1).

[10] Wang, X., & Blaabjerg, F. (2018). Harmonic stability in power electronic-based power systems: Concept, modeling, and analysis. IEEE Transactions on Smart Grid, 10(3), 2858-2870.

[11] Guo, J., Geng, J., Lü, F., & Pan, Y. (2021). Optimisation design of double-column multi-gap reactor core structure for noise reduction. International Journal of Electrical Power & Energy Systems, 133, 107165.

[12] Yuan, F., Lv, K., Tang, B., Wang, Y., Yang, W., Qin, S., & Ding, C. (2021). Optimization Design of Oil‐Immersed Iron Core Reactor Based on the Particle Swarm Algorithm and Thermal Network Model. Mathematical problems in Engineering, 2021(1), 6642620.

[13] Wang, Z., Yu, R., Duan, C., Fan, Z., & Li, X. (2023, September). Analysis of the Vibration Characteristics and Vibration Reduction Methods of Iron Core Reactor. In Actuators (Vol. 12, No. 9, p. 365). MDPI.

[14] Liu, J., & Zhao, Y. (2022, December). Temperature field analysis of dry iron core reactor. In Journal of Physics: Conference Series (Vol. 2401, No. 1, p. 012022). IOP Publishing.

[15] Liao, C., Liu, B., Li, K., & Wang, W. (2024). Accuracy improvement of thermal distribution analysis of 10 kV dry-type iron-core reactor. Case Studies in Thermal Engineering, 64, 105554.

[16] Gao, Y., Ichimaru, S., Miyabe, T., Dozono, H., Muramatsu, K., Guan, W., ... & Chen, B. (2020). Proposal of core structures for iron loss and noise reduction of three-phase reactor with anisotropic iron core. IEEE Transactions on Magnetics, 57(2), 1-5.

[17] Katoch, S., Chauhan, S. S., & Kumar, V. (2021). A review on genetic algorithm: past, present, and future. Multimedia tools and applications, 80, 8091-8126.

[18] Immanuel, S. D., & Chakraborty, U. K. (2019, July). Genetic algorithm: an approach on optimization. In 2019 international conference on communication and electronics systems (ICCES) (pp. 701-708). IEEE.

[19] Gen, M., & Lin, L. (2023). Genetic algorithms and their applications. In Springer handbook of engineering statistics (pp. 635-674). London: Springer London.

[20] Alhijawi, B., & Awajan, A. (2024). Genetic algorithms: Theory, genetic operators, solutions, and applications. Evolutionary Intelligence, 17(3), 1245-1256.

[21] Ascencion-Mestiza, H., Maximov, S., Olivares-Galvan, J. C., Ocon-Valdez, R., Mezura-Montes, E., & Escarela-Perez, R. (2024). Optimization of shunt reactor design using evolutionary algorithms: PSO and DE. Electrical Engineering, 1-11.

[22] Li, Y., Yang, Z., & Guo, P. (2025). Optimal Design of Vibration and Noise for Medium-High Frequency Transformer Core Based on Genetic Algorithm. Journal of Electrical Engineering & Technology, 20(1),

377-387.

[23] T. X. Huang,L. L. Lu,F. G. Chen,Aditya Jain & Y. G. Wang. (2024). Impact of Ni and P substitution for B on the structure and soft magnetic properties of FeBPCuNb amorphous/nanocrystalline alloy. Journal of Materials Science: Materials in Electronics(1),36-36.

[24] Caibo Liao,Bang Liu,Kai Li & Wanqing Wang. (2024). Accuracy improvement of thermal distribution analysis of 10 kV dry-type iron-core reactor. Case Studies in Thermal Engineering105554-105554.

[25] Yuan Fating,Lv Kai,Tang Bo,Wang Yue,Yang Wentao,Qin Shihong & Ding Can. (2021). Optimization Design of Oil-Immersed Iron Core Reactor Based on the Particle Swarm Algorithm and Thermal Network Model. Mathematical Problems in Engineering.

[26] Fang Shi,Hualin Liao,Shuaishuai Wang,Omar Alfarisi & Fengtao Qu. (2025). Optimization of drilling rate based on genetic algorithms and machine learning models. Geoenergy Science and Engineering213747-213747.